

A Survey of Graph-Based Representations and Techniques for Scientific Visualization

Chaoli Wang

University of Notre Dame

Abstract

Graphs represent general node-link diagrams and have long been utilized in scientific visualization for data organization and management. However, using graphs as a visual representation and interface for navigating and exploring scientific data sets has a much shorter history yet the amount of work along this direction is clearly on the rise in recent years. In this paper, we take a holistic perspective and survey graph-based representations and techniques for scientific visualization. Specifically, we classify these representations and techniques into four categories, namely, partition-wise, relationship-wise, structure-wise, and provenance-wise. We survey related publications in each category, explaining the roles of graphs in related work and highlighting their similarities and differences. We also point out research trends and remaining challenges in graph-based representations and techniques for scientific visualization.

Categories and Subject Descriptors (according to ACM CCS): E.1 [Data]: Data Structures—Graphs and networks I.3.6 [Computer Graphics]: Methodology and Techniques—Interaction techniques H.5.2 [Information Interface and Presentation]: User Interfaces—Graphical user interface

1. Introduction

Trees and graphs are well-known structures that use node-link diagrams to represent data relationships. These visual mappings and representations are at the heart of information visualization techniques. Scientific visualization, on the other hand, deals with three-dimensional spatial data that are typically time-varying and multivariate, including scalar and vector quantities. Trees and graphs have long been used to organize and manage scientific data sets for processing and rendering. In these scenarios, they are mostly utilized as an internal data representation.

Over the past decade, we have witnessed the great marriage of scientific visualization and information visualization. Information visualization techniques such as parallel coordinates and treemaps have been successfully utilized to assist a number of scientific visualization tasks including correlation exploration, level-of-detail selection, and transfer function specification. Unlike straightforward applications of parallel coordinates and treemaps that encode co-occurrence and hierarchical relationships among data items, leveraging the more generic and powerful visual means of

graphs often requires a fully integrated pipeline of data transformation, representation, and visual mapping.

Recently, there is a flourishing of works that utilize trees and graphs as visual mappings and interfaces to help scientific visualization tasks. These solutions extract relationships from high-dimensional data over space and time, display these relationships as graphs in a low-dimensional space, and allow users to perform queries and make connection to the original data. This transformative way of exploring scientific data holds the promise to address scientific visualization problems whose size, complexity, and need for closely coupled human and machine analysis may make them otherwise intractable.

We classify related publications in scientific visualization that use trees and graphs into four categories: *partition-wise*, *relationship-wise*, *structure-wise*, and *provenance-wise* representations and techniques. Partition-wise graph representations are concerned with partitioning spatiotemporal data toward effective organization and rendering. These techniques can be traced back to a large body of early work that aimed at fast rendering of large data sets with limited memory available. Relationship-wise graph techniques encom-

	tree	binary tree	quadtree	octree	16-tree	hybrid	graph	directed	undirected	weighted	unweighted	hierarchical	compound	internal	external	w/o interaction	w interaction	combined view	separate view	steady data	unsteady data	scalar field	univariate	multivariate	vector field	others	
partition-wise																											
wavelet tree [GWGS02]			x											x						x		x					
temporal hierarchical index tree [She98]	x													x						x		x					
BONO [WVG92]			x											x						x		x					
multi-dimensional trees [WVG94]	x													x						x		x					
TSP tree [SCM99]						x								x						x		x					
WTSP tree [WS04]						x								x						x		x					
multiresolution video [FJS96]						x								x						x		x			x		
SPT tree [DCS09]						x								x						x		x					
binary swap [MPH94]		x												x											x		
2-3 swap [YWM08]	x													x											x		
hierarchical navigation interface [WS05]						x										x	x			x		x			x		
LOD map [WS06a]			x													x	x			x		x			x		
relationship-wise																											
iTree [GW13]	x													x	x	x			x		x						
Multifield-Graphs [STS06]								x	x	x						x	x			x		x			x		
attribute cloud [JBS08]								x	x							x	x			x		x			x		
ε-machine [JS09]						x	x									x	x			x		x			x		
TransGraph [GW11]							x	x	x							x	x			x		x					
Flow Web [XS10]							x	x	x							x	x			x					x		
FlowGraph [MWSJ14]							x	x	x	x						x	x			x		x			x		
binary connectivity graph [BSL*14]								x	x							x	x			x					x		
feature correspondence graph [SSZC94]								x	x							x				x		x					
Petri Nets [OSBM14]								x	x							x				x		x					
flow graph [NLS11]								x	x							x				x		x			x		
access dependency graph [CNLS12]								x	x							x				x					x		
structure-wise																											
contour spectrum [BPS97]	x															x	x			x		x			x		
contour tree interface [CSvdP04]	x															x	x			x		x			x		
skeleton tree [GKHS98]	x															x				x		x			x		
volume skeleton tree [TTFN05]	x															x				x		x			x		
topological landscape [WBP07]									x								x	x			x				x		
cancellation tree [BPH05]	x															x				x		x			x		
topological spine [CLB11]									x								x	x			x				x		
empty region graphs [CL11]									x											x		x			x		
topology change graph [SB06]							x										x	x			x			x			
attributed relational graph [MBB*12]								x	x								x	x			x				x		
augmented extremum graph [TN13]									x							x				x		x			x		
extended BDG [SSW14]															x					x		x			x		
relation graph [CQC*08]																	x	x			x			x			
saddle connectors [TWH03]																		x			x				x		
joint contour net [CD14]																	x	x			x			x			
simplicial chain graphs [RL14]									x	x							x	x			x				x		
provenance-wise																											
image graph [Ma99]																	x	x			x				x		
spreadsheet-like interface [JKM01]																	x	x			x				x		
derivation graph [JKMG02]																	x	x			x				x		
volume tree [WS06b]	x																x	x			x				x		
storyboard [LS08]	x																x	x			x				x		
event graph [YLRC10]																	x	x			x				x		
VisTrails [BCC*05]																	x	x								x	
interaction graph [GS06]																	x	x								x	

Figure 1: Selected tree and graph representations from the four categories.

pass similarity-based hierarchical data clustering, various relationship graphs based on correlation, transition or correspondence, as well as general- and special-purpose trees and graphs for parallel and out-of-core visualization algorithms. Structure-wise graph techniques mainly study topological structures of data which can be treated as a special case of relationship-wise graph techniques. We separate them into a different category due to a variety of topological trees and graphs applied to scalar, vector and multifield data visualization. Finally, provenance-wise graph representations deal with visualization history and parameter management, storytelling, animation creation, and reproducible visualization.

1.1. Scope of Survey

To collect related publications for this survey, we started with the collection of papers we knew of from our own research, then scanned through three major visualization conferences (*IEEE Visualization Conference, Eurographics Conference on Visualization, IEEE Pacific Visualization Symposium*) and two major visualization journals (*IEEE Transactions on Visualization and Computer Graphics, Computer Graphics Forum*) to identify related papers.

The criteria for us to select a paper are that the work is relevant to tree and graph based representations and techniques,

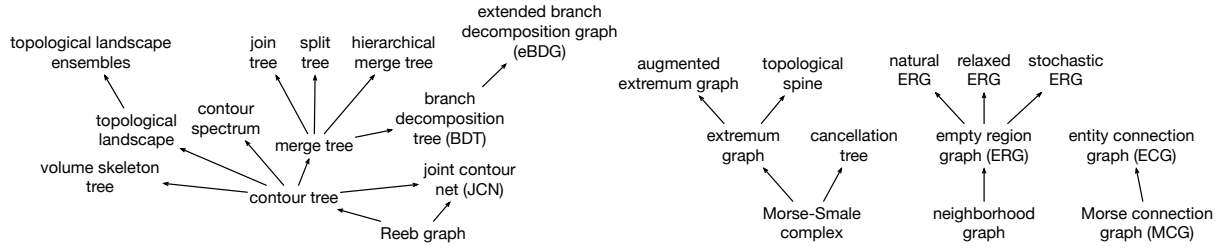


Figure 3: Various trees and graphs for structure-wise graph representations and techniques. The arrow line represents a variant, extension, or special case.

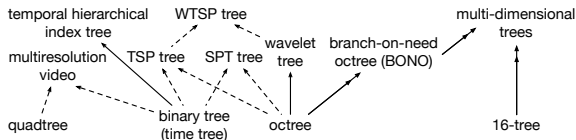


Figure 2: Various trees for partition-wise graph representations and techniques. A solid line with single arrow head represents a variant, extension, or special case while a solid line with double arrow heads represents a generalization. Dashed lines represent a combination.

and the work is within the context of scientific visualization. Therefore, the large collection of graph visualization papers in information visualization is not included. We also omit the works that transform scientific data into different kinds of scatterplots or projections using techniques such as principal component analysis (PCA) and multidimensional scaling (MDS) since there is no explicit edges defined to construct the graph view. Furthermore, we do not survey graph drawing and layout algorithms, but focus on their application and utilization in scientific visualization. We refer readers to the following survey papers [HMM00, vLKS*11, BBDW14] for graph visualization, large graph analysis, and dynamic graph visualization.

Needless to say, including all relevant publications is beyond the scope of this survey. For example, as a general data structure, the octree has been widely used for partitioning 3D volume data. As such, we only picked a small collection of representative papers in this direction. Furthermore, we gave higher priority to new and interesting use of graph techniques for visual representation and navigation than conventional use of well-known tree and graph structures for data organization and management. Finally, some graph representations, such as Reeb graphs, have found a wider variety of applications in other fields such as computer graphics and computational geometry instead of scientific visualization. We therefore briefly mentioned these representations rather than giving an extensive review.

1.2. Overview of Different Representations

To help readers gain an overview of various trees and graphs surveyed, we list selected tree and graph representations from the four categories in Figure 1, pointing out their respective tree or graph types, representation modes, and kinds of data handled. For partition-wise and structure-wise techniques, we further illustrate the relationships among different trees and graphs in Figures 2 and 3, respectively. We do not present such an illustration for relationship-wise or provenance-wise techniques. This is because they either have a much broader range of topic (relationship-wise) which makes the illustration inadequate or have a much narrower scope of focus (provenance-wise) which makes the illustration unnecessary.

2. Partition-wise Representations and Techniques

Many of the early research efforts in scientific visualization leveraged tree-like structures to organize and manage three-dimensional volumetric data. The main idea is to create a tree hierarchy by recursively subdividing the domain and preparing data with different resolutions for compression, representation and visualization. Such a hierarchical structure allows us to use low resolution data for regions with low importance in order to speed up the subsequent processing and rendering. As a matter of fact, the same idea has been widely used in image and video processing, albeit in lower dimension. One can build such tree structures in any dimension while the most common forms are in 1D to 4D: binary tree (1D), quadtree (2D), octree (3D), and 16-tree (4D). These trees are normally built from 1D signal or time series, 2D image, 2D video or 3D volume, and 3D time-varying volume, respectively. For 2D video data, the third dimension of time t is treated equally as the two spatial dimensions x and y . Likewise, for 3D time-varying volume data, the fourth dimension of time t is treated equally as the three spatial dimensions x , y and z .

In its simplest form, the domain is *evenly* partitioned along each dimension *simultaneously* and the partitioning planes are always aligned with the corresponding coordinate axes. In practice, we often introduce several variations to improve the flexibility, efficiency and effectiveness of such solutions. First of all, the partition could be adaptive. For ex-

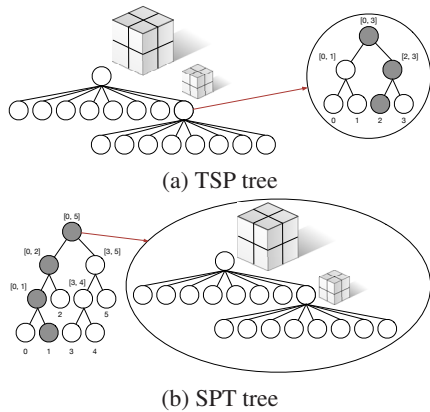


Figure 4: Illustration of TSP and SPT trees. (a) an example of the TSP tree with four time steps. (b) an example of the SPT tree with six time steps.

ample, we do not partition a region further if the data within the region meet certain criteria (e.g., the error within the block is less than a given threshold or the block has reached the minimum block size). This saves unnecessary partitions and is thus more efficient. Second, the partition could be uneven or could follow one axis at a time. For the former case, we can adjust the partition based on data properties and produce a tighter partitioning, yielding a tree with less hierarchical levels. For the latter case, we would produce a partitioning similar to the *k-d tree*. These strategies are adopted if we want to have a similar number of data elements or items in each leaf node of the tree in order to speed up the subsequent searching or indexing. Third, the partition does not have to be axis-aligned. This leads to *binary space partitioning trees* (BSP trees) which are more general than *k-d trees* as partitioning planes may have any orientation rather than being aligned with the coordinate axes.

2.1. Standard Tree Structures

In volume visualization, standard octree structures have long been used for data encoding and rendering. An early work of Meagher [Mea82] uses octree encoding for geometric models and volumetric data. Levoy [Lev90] utilized a binary octree to skip empty regions for efficient ray tracing of volume data. Laur and Hanrahan [LH91] stored the volume data using an octree, sorted the cells from back to front, and calculated cell projections for hierarchical splatting. LaMar et al. [LHJ99] used an octree hierarchy for texture-based volume rendering where the octree nodes store volume blocks resampled to a fixed resolution and rendered using 3D texture hardware. Boada et al. [BNS01] presented an octree-based structure for multiresolution volume visualization where the hierarchical texture memory representation and management policy benefits nearly homogeneous regions and regions of lower interest. Carmona and Froehlich [CF11] designed a greedy, real-time cut update algorithm based on split-and-

collapse operations for octree-based multiresolution volume raycasting using GPU.

Different data reduction and compression schemes have also been incorporated into octree-based volume visualization. Examples include *Laplacian pyramids* [GY95], *wavelet trees* [GWGS02, GWLS05], application-driven compression [WYM10], and tensor approximation and reconstruction [SIGM*11, SMP13].

The common way to partition the time dimension is to iteratively partition the time span into half to build a binary tree. For instance, the *temporal hierarchical index tree* [She98] is a structure for creating the isosurface cell search indices from a time-varying field. Cells are characterized based on their extreme values and the variations of the extreme values over time. Cells that have a small amount of variation over time are placed in a single node of the tree that covers the entire time span. Cells with a larger variation are placed in multiple nodes of the tree multiple times, each for a short time span. The temporal hierarchical index tree requires much less storage space and significantly reduces the amount of I/O required to access the indices from the disk at different time steps.

For time-varying volume data visualization, Ma and Shen [MS00] used octree encoding and difference encoding for spatial and temporal domain compression, respectively. Linsen et al. [LPD*02] presented a four-dimensional multiresolution approach that supports a hierarchy with spatial and temporal scalability. In their scheme, temporal and spatial dimensions are treated equally in a single hierarchical framework. Similar uniform treatments of space and time have been used for representing and visualizing time-varying 3D vector fields [YWM07, MWSJ14]. Different from the normal way of evenly partitioning the space, the *branch-on-need octree* (BONO) [WVG92] partitions the dimension non-uniformly to avoid empty regions. *Multi-dimensional trees* [WVG94] extend the BONO to multi-dimensional data sets, such as spatiotemporal data.

2.2. Hybrid Tree Structures

Applying the 4D tree or 16-tree to organize time-varying volume data treats time merely as another “spatial” dimension. Although simple to implement, the 16-tree could be ineffective for two reasons. First, there could be large discrepancy between the spatial and temporal dimensions, which makes it difficult to subdivide the spatial and temporal dimensions uniformly without over partitioning. Second, in 16-trees, the temporal and spatial domains are tightly coupled in the hierarchical subdivision. This implies that it could be difficult to choose a flexible combination of spatial and temporal data resolutions from the 4D hierarchy.

To remove the dependency between spatial and temporal resolutions, researchers proposed different hybrid tree structures. Shen et al. [SCM99] introduced the *time-space partitioning tree* (TSP tree), a time-supplemented octree for or-

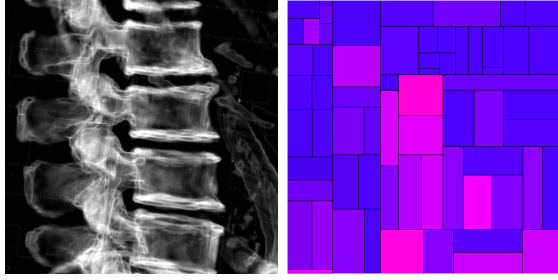


Figure 5: A zoom to the spine of the visible woman data set and the corresponding LOD map showing the LOD quality. In the LOD map, the contribution of a data block to the final image is mapped to the size of the corresponding rectangle, while the distortion is mapped to the color (magenta to blue for large to small distortion). Images © 2006 IEEE. Reprinted with kind permission from Wang and Shen [WS06a] and IEEE.

ganizing a time-varying volume data. As sketched in Figure 4 (a), the skeleton of a TSP tree is a standard complete octree, which recursively subdivides the volume spatially until all subvolumes reach a predefined minimum size. In each of the TSP tree nodes, a binary time tree is created, where each node in the binary time tree represents a spatial subvolume with a different time span. Each time tree node stores the mean voxel value as well as spatial and temporal errors of the subvolume in the given time span. These values are used for tree traversal during the volume rendering process. The unique advantage of TSP tree is that it allows users to request spatial and temporal data resolutions *independently* with separate error thresholds. In this way, a flexible browsing of data at arbitrary spatiotemporal resolutions becomes possible. Wang and Shen [WS04] integrated wavelet transform and compression with the TSP tree and presented the *wavelet-based time-space partitioning tree* (WTSP tree) for managing large-scale time-varying data hierarchically.

When partitioning both space and time domains hierarchically to explore spatial and temporal coherence in time-varying data, one could either partition the spatial domain or the temporal domain first. The TSP tree chooses to partition the spatial domain first in order to maintain the visibility order and spatial locality among the subvolumes during the tree traversal. On the contrary, Finkelstein et al. [FJS96] introduced *multiresolution video* by partitioning the temporal domain first, creating the primary binary time tree. For each time tree node, the spatial domain is then partitioned into a quadtree. Du et al. [DCS09] studied the open question of which domain should be partitioned first for a better data reuse rate. They showed both theoretically and experimentally that partitioning the time domain first is better. They further presented the *space-partitioning time tree* (SPT tree) which has the fully balanced binary time tree as the primary structure and a standard complete octree as the secondary

structure, as sketched in Figure 4 (b). Compared to the rendering based on the TSP tree, volume rendering based on the SPT tree has the following advantages. First, it leads to a higher level of details since the algorithm is more likely to select smaller but more subvolumes. Second, it has a higher reuse rate because the algorithm favors higher-level time tree nodes. Third, the algorithm runs faster thanks to the higher reuse rate.

2.3. Parallel Image Compositing

Ma et al. [MPH94] introduced the classical *binary swap* algorithm for parallel image compositing. The algorithm works in multiple stages. It makes use of all processors in each stage of composition in a binary tree fashion. For N processors, the number of stages required is $\log N$. At each stage, the image space is divided into two partitions and each processor takes the responsibility for one of the two partitions. A swapping of the partitions between the two processors is needed, thus the name binary swap. Due to the nature of binary compositing, the binary swap algorithm may not work well when the number of processors is not an exact power-of-two. Yu et al. [YWM08] presented a generalized image compositing algorithm called the *2-3 swap* which works with an arbitrary number of processors. This flexibility is achieved by allowing each node in the compositing tree to have either two or three children. The resulting *2-3 tree* is a balanced tree, which defines the structure of the compositing tree and determines the grouping of processors during each stage of image compositing.

2.4. Visual Mapping and Interface

Most partition-wise representations of volumetric data record tree structures *internally* in memory for level-of-detail (LOD) querying and rendering. Only a few research works present such a tree *externally* as a visual mapping as well as an interface for LOD selection. Examples of these external tree mappings include the hierarchical navigation interface [WS05] and LOD map [WS06a] presented by Wang and Shen. Both works utilize the treemap representation. The treemap [Shn92] is a space-filling method for visualizing large hierarchical information (in this case, the current LOD, or a cut through the tree hierarchy). It works by recursively subdividing a given display area based on the hierarchical structure, and alternating between vertical and horizontal subdivisions. The information of an individual node is presented through visual attributes, such as color and size, of its bounding rectangle.

The *hierarchical navigation interface* [WS05] works with the WTSP tree representation of a time-varying data set and has two views. The first view is an overview map illustrating the tree hierarchy in a triangle shape, the error distribution among tree nodes, and the current LOD as a cut through the hierarchy. The second view is the treemap showing the detail node information in the current LOD in an uncluttered view which helps users pinpoint the target regions.

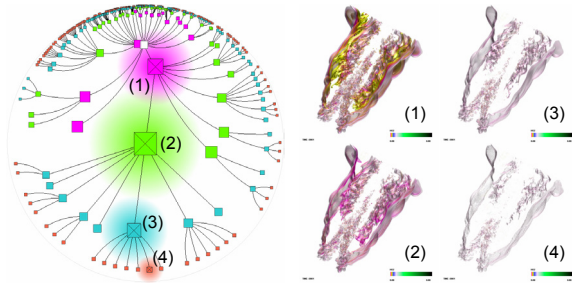


Figure 6: Level-of-detail exploration of the *iTree* of the combustion data set. Four nodes at different levels of detail in the tree are selected and their corresponding clusters are highlighted in the volume. Images © 2013 IEEE. Reprinted with kind permission from Gu and Wang [GW13] and IEEE.

The *LOD map* [WS06a] leverages a treemap to guide multiresolution volume rendering using the wavelet tree representation. It supports effective LOD volume visualization through a suite of functions including LOD comparison, view comparison, LOD adjustment, and budget control (i.e., giving a LOD of similar quality but with a reduced block budget). An example result of LOD map is shown in Figure 5. The benefits of these explicit visual representations are two folds. First, they provide the *complete* information about the LOD quality of multiresolution data blocks which is impossible to get from the rendering due to the projection of a 3D volume to a 2D image. Second, they also serve as visual interfaces which enable users to interactively adjust the LOD in a guided and controllable fashion.

3. Relationship-wise Representations and Techniques

Relationship is a general term that could refer to any kind of relation among nodes in a tree or graph. Similar to many other applications, the most common way to form a tree-like hierarchy in scientific visualization applications is to either cluster data items from bottom up or partition an object from top down, based on certain similarity or distance measures. For time-varying multivariate data, relationships could mean transition relations, correlation relations, etc. Relationships could also be domain-specific or application-specific. Feature extraction and tracking is an important task for time-varying data visualization and the extracted features are normally connected through a correspondence graph. In addition, different tree and graph structures have also been built for data distribution, task partition, and workload prediction for parallel and out-of-core visualization algorithms.

3.1. Hierarchical Clustering or Partitioning Trees

Linsen et al. [LLRR08] used a cluster tree to represent the level-of-detail of the surfaces constructed from multivariate particle data. They converted the multifield particle volume data to a high-dimensional feature domain, partitioned the domain into cells, and derived the cell density. Then they

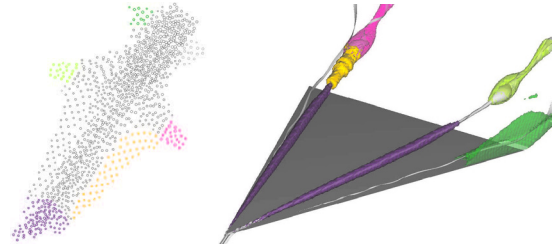


Figure 7: Analogue brushing with six variables of the multivariate delta wing data set using the attribute cloud. The six variables are the norm of velocity, pressure, density, x -, y -, and z -coordinate of position. Images © 2008 IEEE. Reprinted with kind permission from Jänicke et al. [JBS08] and IEEE.

clustered the cells into to a high density cluster tree where each cluster corresponds to a surface representing the particles within the cluster. Finally, they employed 3D star coordinates to visualize nested density clusters as surfaces.

Ip et al. [IVJ12] utilized a tree-based representation to help users explore a 3D intensity field adaptively. They converted the 3D intensity field into a 2D intensity-gradient histogram and applied the normalized cut algorithm to partition the histogram into segments. By iteratively partitioning the histogram, they created a tree hierarchy which records the level-of-detail partition process. The tree serves as an interface for users to explore the embedded structures. Günther et al. [GRT14] also utilized a tree structure to store streamline clustering information for a 3D vector field. With this tree, users can set opacities for different streamline segments to reduce visual occlusion and clutter and highlight regions of interest. To this end, they first evenly partitioned all streamlines into segments, then used a binary tree to cluster stream segments into a hierarchy. A good streamline visualization result can be achieved by assigning different opacity values to subtrees and optimizing the global opacity.

Gu and Wang [GW13] introduced *iTree* for time-varying data visualization, which integrates data classifying, indexing and compacting into a single framework. They utilized the symbolic aggregate approximation (SAX) for data compacting and indexable SAX (iSAX) for indexing. Although iSAX is already stored internally as a tree structure, it is difficult to visualize and interact due to its wide branching and high depth. To convert iSAX to a user-friendly user interface, they performed level promoting, sibling grouping, and sibling reordering to reduce the width and height of the iSAX tree. The resulting visual interface, *iTree*, uses a hyperbolic layout for focus+context visualization and provides direct interactions for users to query, search and track the time-varying volumetric data. An example of level-of-detail exploration of the *iTree* is shown in Figure 6.

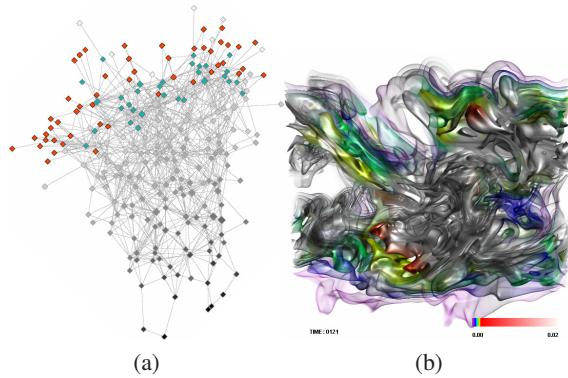


Figure 8: *TransGraph* query of the combustion data set. (a) nodes that are only involved in self-transition are in red and the rest of nodes at the same time step are in green. (b) volume highlighting corresponds to the red nodes. Images © 2011 IEEE. Reprinted with kind permission from Gu and Wang [GW11] and IEEE.

3.2. Relationship Graph Encoding and Visualization

Graphs can be used to encode the relationships between variables. In such a graph, a node simply represents a variable and an edge represents the relationships between variables. Therefore, these graphs are typically fully connected. For instance, Qu et al. [QCX*07] built an undirected weighted graph to visualize the correlation between variables. Biswas et al. [BDSW13] leveraged the same kind of graph to encode the mutual information between variables. These two graphs are drawn using a force-directed layout. Wang et al. [WYG*11] studied the information transfer between variables. Since information flow carries directional information, they utilized a directed weighted circular graph to show the information transfer between variables. Oeltze et al. [OFH*11] applied graph visualization techniques for visual analysis of high-dimensional, multi-parameter fluorescence microscopy data. They drew a circular graph where each node represents an affinity reagent while each edge represents two co-occurring affinity reagent bindings.

Besides using a node to represent a variable in the graph, other solutions use a node to represent spatiotemporal data blocks, derived fields, or other quantities. This leads to more refined results of graph relation since a node now represents a group of voxels rather than an entire variable or time step. The graph could be *hierarchical* so that the relationships can be shown in a coarse-to-fine manner. Furthermore, the graph could also be *compound* with different kinds of nodes and edges encoding more complex data relationships.

For multivariate data visualization, Sauber et al. [STS06] developed *Multifield-Graphs* for a complete visualization of scalar fields and their correlations so that features associated with multiple fields can be discovered. In *Multifield-Graphs*, a node denotes the correlation field among variables. An

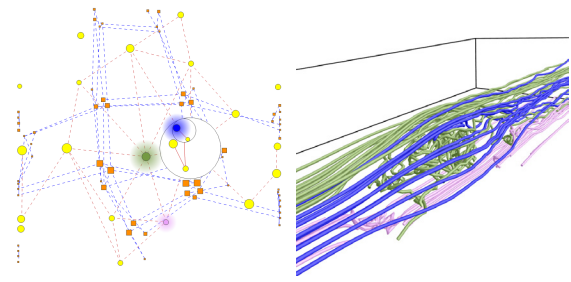


Figure 9: Selecting three *L*-nodes in the car flow data set using *FlowGraph* to capture the main flow structure passing through the car. Images © 2013 IEEE. Reprinted with kind permission from Ma et al. [MWS13] and IEEE.

edge connects a parent and its immediate child if and only if the parent node has one new variable in the correlation field than that of the child node. The graph allows both correlation overview and focused display of certain nodes. A limitation of *Multifield-Graph* is that the number of nodes in the graph increases exponentially with the number of dimensions. Jänicke et al. [JBS08] transformed multivariate data from their high-dimensional attribute space to a 2D *attribute cloud* by constructing the minimum spanning tree (MST) from sample points in the original high-dimensional space and utilizing a graph layout algorithm to minimize edge crossings in 2D. Through brushing and linking the attribute cloud with the data, users can conveniently connect the abstract attribute space with the original data space. An example of brushing the attribute cloud and the corresponding volume highlighting is shown in Figure 7.

For time-varying data visualization, Jänicke and Scheuermann [JS09] introduced a directed graph representation named the ϵ -*machine*. Leveraging a light-cone structure, they defined a causal state as all the required information in a given position to predict its future. Transition probabilities among states can be derived based on transition frequencies. In the ϵ -*machine*, a node represents a causal state and a directed edge connecting two nodes represents their transition probability. Gu and Wang [GW11] designed *TransGraph* to visualize the transition relationships in a time-varying volumetric data set. In *TransGraph*, a node denotes a state, i.e., a spatiotemporal region, and a directed edge between two nodes indicates their transition probability. *TransGraph* organizes the states hierarchically and the resulting hierarchical graph enables relationship overview and detail exploration of a 4D time-varying volume data set in a single 2D graph view. Figure 8 gives such an example.

For flow visualization, Xu and Shen [XS10] introduced the *Flow Web*, which provides an overview of the 3D flow field and help users locate regions of interest. To construct the *Flow Web*, they first partitioned the volume into regions using an octree. Then they performed random seeding in each region to trace streamlines. In the *Flow Web*, a

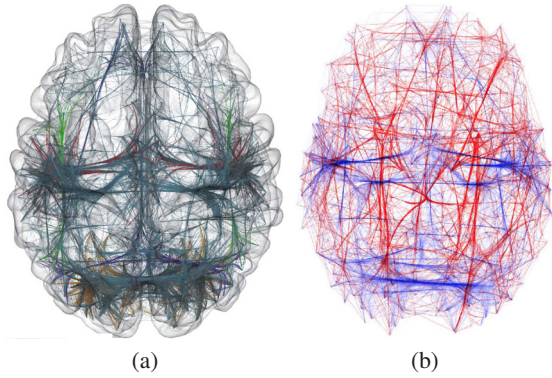


Figure 10: Brain connectivity graphs. (a) the whole-brain group-level connectivity with the bundled graph. (b) the comparison between functional (blue) and anatomical (red) connectivity. Images © 2014 IEEE. Reprinted with kind permission from Böttger et al. [BSL*14] and IEEE.

node represents a region and a weighted edge between two regions indicates the number of streamlines going through them. To allow for easy understanding of the underlying flow structures, they created hierarchical Flow Webs by splitting or merging nodes and edges. Rather than only considering streamline clusters or spatial regions as nodes, *FlowGraph* developed by Ma et al. [MWS13] integrates both streamline clusters or spatial regions as nodes and thus presents a more complete picture. As a *compound* graph, *FlowGraph* consists of two kinds of nodes (L-nodes and R-nodes) and three kinds of edges (L-L edges, R-R edges, and L-R edges) where ‘L’ denotes streamline and ‘R’ denotes spatial region. To construct the hierarchical graph, they clustered streamlines hierarchically from bottom up and partitioned spatial regions recursively from top down. A set of functions is designed to enable hierarchical exploration of streamline clusters, spatial regions and their interconnection, detail comparison among streamline clusters, and close examination of spatial regions. Figure 9 shows an example of exploring interesting flow patterns using *FlowGraph*. Ma et al. [MWSJ14] further extended *FlowGraph* to analyze and visualize the relationships between pathlines and spatiotemporal regions in 3D unsteady flow fields.

Studying the anatomical and functional connectivity within a brain is an important topic in neuroscience. The derived connectivity graphs are undirected and unweighted. Beyer et al. [BAAK*13] presented *ConnectomeExplorer*, where a *connectivity graph* was used to visualize the connections among axons or dendrites. In the 2D connectivity graph view, nodes correspond to axons or dendrites, and edges represent synapses between them. Böttger et al. [BSL*14] used a *binary graph* in conjunction with an edge bundling technique to show the group-level connectivity information within a whole brain. In the binary graph, nodes represent cortical parcels and edges indicate strongly connected nodes.

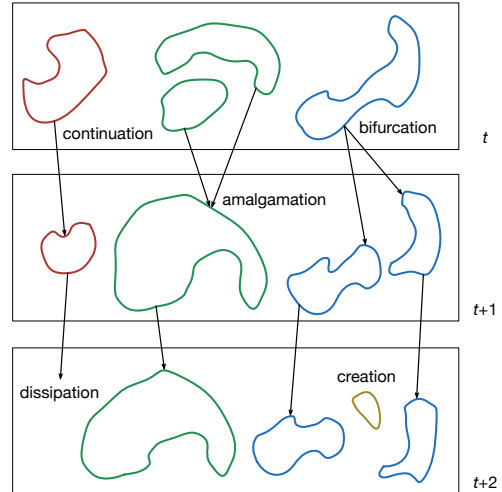


Figure 11: Different feature tracking events: continuation, bifurcation and amalgamation for matched features, and creation and dissipation for unmatched ones.

In Figure 10, two binary bundled graphs show the whole-brain connectivity information. Unlike previous examples of *iTree*, attribute cloud, *TransGraph* and *FlowGraph* shown in Figures 6 to 9, the connectivity graphs are drawn in the 3D spatial domain so the contextual brain information is retained. The edge bundling technique is applied to produce a less cluttered view.

3.3. Feature Correspondence and Tracking

An important task for time-varying data analysis and visualization is feature extraction and tracking. An early work by Samtaney et al. [SSZC94] extracts features (i.e., regions that fulfill certain criteria) and makes correspondence in neighboring time steps. The features are matched through their attributes such as the centroid, volume and mass. For the neighboring two time steps, they compared every feature pair for a possible match. If there is a match, then the two features are corresponded based on the relation of continuation. After removing all the continuous features, they compared the combination of multiple features to test for bifurcation or amalgamation cases. The remaining unmatched features are considered to be dissipation or creation. Figure 11 illustrates these five different events commonly identified in feature tracking. The evolution of features over time can be mapped to a directed acyclic graph (DAG) which records feature correspondence.

A limitation of the work by Samtaney et al. [SSZC94] is that since all feature combinations need to be considered for the decision of bifurcation and amalgamation, the computation cost remains high. To reduce the cost of comparing all the feature combinations, Silver and Wang [SW97] utilized octrees to store all the features, which allows fast identification of feature overlapping in space. Spatial overlap is used

to determine feature matching. For a selected feature in one time step, they found out those candidate features in the next time step which overlap it. Then they applied a normalized volume difference test to choose the best matching from the candidates.

Commonly used approaches for feature extraction include region growing with a certain threshold or extracting the iso-surfaces with a given isovalue. Woodring and Shen [WS09] found the features at each time step using a k -means clustering algorithm. For each time step, they first generated k clusters based on the input time-activity curves within a time interval. Then they created a directed graph that connects the clusters over time. To find the links between features, they estimated the probability of transferring one feature to another by computing the distance of their time histograms.

The recent work of Ozer et al. [OSBM14] advances the state-of-the-art feature tracking by leveraging *Petri Nets* to model and detect activities in scientific visualization. Petri Nets are graph-based techniques that model and visualize various types of behaviors. The Petri Nets model includes places (types of possible object states), transitions (conditions or actions between places), and directed arcs (connections between places and transitions). Based on the results of feature extraction and tracking, they utilized Petri Nets to model the activity of interest and ran the algorithm for hypothesis validation.

3.4. Parallel Processing and Visualization

Trees and graphs have also been designed to facilitate data distribution and task partitioning for high-performance parallel visualization applications. For parallel visualization of 3D unsteady flow fields, Yu et al. [YWM07] constructed a hierarchical 4D representation of the spatiotemporal data so that pathline tracing can be treated as streamline tracing in 4D. They built an adaptive grid for hierarchical vector field clustering. The clustering merges neighboring grid cells of similar patterns and yields a binary cluster tree. At runtime, they traversed the binary cluster tree to obtain the seeds from the clustering of the adaptive grid representation. The streamlines are then traced in parallel in the original 4D vector data to generate pathline results.

For parallel feature extraction and tracking, Wang et al. [WYM13] presented a solution that extracts local partial features at individual processors and then integrates partial features based on the connectivity information to extract and track features in parallel. Specifically, for each block, they created a *local connectivity tree* with six children corresponding to its six spatial neighboring blocks. The processor associated with its assigned block communicates with its neighbors to exchange the centroids and the minimal and maximal region boundaries of the features. Such information is used to match the features with the neighbors in the current time step. Then, based on the local connectivity trees, they created a *global connectivity graph* to store the information

of all the features in that time step. This process repeats for the subsequent time steps. Since features normally change little in neighboring time steps, feature movements could be identified through their movements between processors in the global connectivity graph.

For parallel streamline generation, Nouanesengsy et al. [NLS11] designed the *flow graph*, a directed weighted graph to estimate the workload for each data block. They followed the work of Flow Web [XS10] for blockwise data partitioning and random seed placement. While the Flow Web counts the number of particles traveling through the boundaries of blocks, the flow graph calculates the corresponding probabilities and treats them as edge weights. The resulting graph guides the estimation of particle movements. The flow graph only stores the information of traveling through blocks. No information of traveling within each block, such as the lengths of streamlines in the block, is kept. During each round of tracing, the algorithm also considers the average number of tracing steps per particle for more accurate workload estimation and balancing.

3.5. Out-of-Core Field Line Tracing

For out-of-core streamline tracing, Chen et al. [CXLS12] developed the *access dependency graph* (ADG) to guide data reorganization with the goal of reducing the I/O miss ratio. In an ADG, a node represents a spatial data block, and an edge connects two blocks if there are particles traveling between them. Besides spatially adjacent blocks, the ADG also considers non-adjacent blocks if they are on the same flow path of a particle. A linear ordering of data block files is required for I/O performance optimization so that when a file is needed and uploaded to main memory for streamline tracing, its neighboring files would also be fetched to reduce the I/O cost. Therefore, an appropriate reordering of files could reduce the miss ratio. Unlike the flow graph [NLS11] which only uses one-hop prediction, the ADG considers N -hop in the prediction and the final ADG is the union of graphs G_1 to G_N . They formulated the optimal layout problem as a graph linear arrangement problem. The miss ratio is minimized when the sum of distances in the file for data blocks along the same flow paths is minimal.

Chen et al. [CNLS12] further extended the ADG for out-of-core pathline tracing. Each node in the ADG is called a time block which consists of the blocks at the same location in a time period. A directed edge connects two time blocks if there exists pathlines passing through them. Each edge is assigned a weight equal to the probability of seeds moving from one block to the other. The finite-time Lyapunov exponent (FTLE) helps users study the existence of the Lagrangian coherence structures (LCS) by quantifying the separation of flows. However, in order to produce a high-resolution FTLE field, we need to trace a pathline from every grid point and at every time step, which is very time-consuming. Chen and Shen [CS13] presented an out-of-core solution for efficient FTLE and pathline computa-

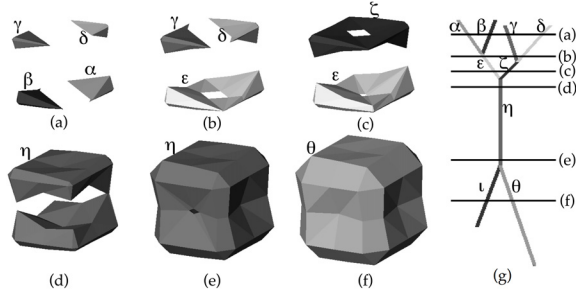


Figure 12: The contour tree with horizontal lines corresponding to level sets (a) to (f) produced at six distinct points during sweep from high to low isovalue. Note that in (f), contour η is separated into invisible inner (ι) contour and visible outer (θ) contour. Image reprinted with kind permission from Carr [Car04].

tion through reducing I/O cost and maximizing data reusing. They first utilized the ADG to estimate the tracing probabilities between neighboring blocks and then applied the discrete-time Markov chains on the ADG to predict the probabilities between all the blocks. Finally, they performed seed scheduling to select and order the seeds for tracing at each round to maximize the usage of data blocks.

4. Structure-wise Representations and Techniques

Scientific visualization often deals with discrete data sets with values sampled at grid points in a volume. Extracting the structural information from discrete data is critically important toward efficient understanding of the underlying data. For instance, there is a large body of work on the model-based visualization of vascular structures in medical visualization [PO08]. Vasculature is represented and analyzed by means of a *branching graph* [HPSP01].

Topology refers to a structure imposed upon a data set that essentially characterizes properties of space such as convergence, connectedness and continuity. Topology-based methods provide a concise and rigorous description of the overall structure and lead to mathematically sound tools for processing, exploration and visualization of scientific data sets. Topological methods based on *Morse theory* include several abstract representations for studying scalar fields: contour trees, Reeb graphs, and Morse-Smale complexes. Morse theory shows that topological changes in scalar field data defined on manifolds occur at distinct isolated points, i.e., *critical points*. The *Reeb graph* shows the evolution of individual contours using these critical points and their relationships. The *contour tree* is a representation that records changes in the topology of the *level sets* (i.e., isocontours) of a scalar field. It is a special case of the Reeb graph where the graph forms a tree structure for simply connected domains. The *Morse-Smale complex* is a partition of the domain into cells according to the gradient of the scalar field. In this survey,

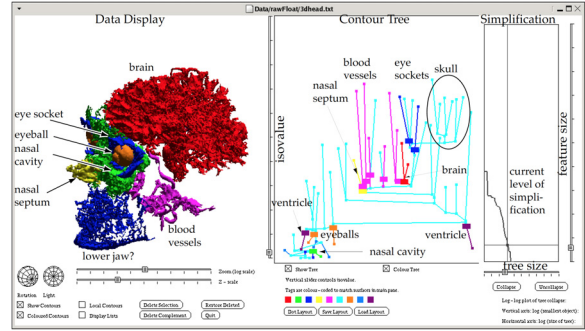


Figure 13: A flexible isosurface chosen from a simplified contour tree. The rightmost pane controls the amount of simplification of the contour tree shown immediately to its left. The interface supports interactive exploration of structures that are hidden in the conventional view. Image © 2004 IEEE. Reprinted with kind permission from Carr et al. [CSvdP04] and IEEE.

we restrict our attention to contour trees since they are most widely used in scientific visualization applications.

The contour tree captures the topological evolution of an isosurface as the isovalue changes. Since the domain is simply connected, it does not contain loops. As shown in Figure 12, in a contour tree, nodes represent critical points where the number of components varies. Critical points have three classes: *minima*, *maxima* and *saddles*. Leaf nodes are *extrema* (i.e., minima and maxima) representing the creation or deletion of components. Interior nodes are saddles representing the joining or splitting of two or more components. An arc represents contours between critical points, i.e., contours which do not change topology as the isovalue varies between critical values. The value difference of two nodes along an arc is called *persistence* which measures the importance of the corresponding topological features.

The contour tree can be created by first scanning the data set twice: one pass to create the *join tree* and the other pass to create the *split tree*, and then merging the join and split trees together [CSA03]. A *merge tree* (i.e., a join or split tree) is a substructure of contour trees that tracks either merges or splits of the isocontours.

4.1. Contour Trees

As an abstraction of a scalar field that encodes the nesting relationships of isosurfaces, the contour tree has been used to accelerate isosurface extraction, to identify salient isovalues, and to guide exploratory visualization.

Bajaj et al. [BPS97] introduced the use of *contour spectrum* for exploring complex scalar fields. The contour spectrum provides an interface which plots properties such as isosurface area and enclosed volume, along with the contour tree, for users to explore interesting isosurfaces. Carr et

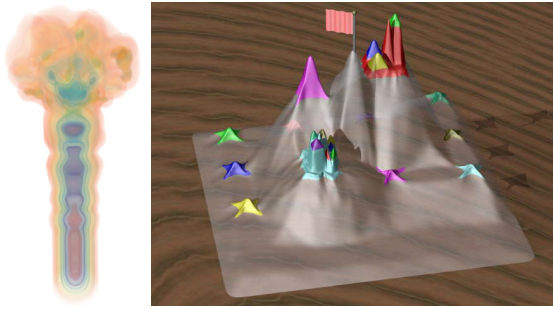


Figure 14: The topological landscape of the fuel data set. Peaks correspond to maxima and valleys correspond to minima. The main mountain is presented in a semi-transparent gray to facilitate the visualization of deep valleys and its center is marked by a flag. Images © 2007 IEEE. Reprinted with kind permission from Weber et al. [WBP07] and IEEE.

al. [CSvdP04] designed an effective contour tree simplification algorithm that computes local geometric measures for individual contours and uses them to suppress minor topological features in the data. The contour tree is simplified with two operations: leaf pruning and vertex reduction. As shown in Figure 13, they presented a flexible isosurface interface to explore individual contours interactively. Carr et al. [CSvdP10] presented an interface that allows users to select an individual contour for manipulation. The contour can be selected from the contour tree or the isosurface display. A set of functions such as contour removal, contour evolution, and contour tracking is provided. These functions are realized based on the attaching of isosurface seeds (i.e., path seeds) to each edge of the contour tree so that individual contours can be extracted on demand.

Galvani et al. [GKHS98] presented a solution for volume animation using the *skeleton tree*. They extracted skeletal voxels and connected them to form a graph based on spatial closeness and value similarity. The minimum spanning tree is extracted from the graph to yield the skeleton tree, which suggests the shape of the object. Using line segments to connect skeletal voxels, one can generate a skeletal structure that is amenable for intuitive motion and deformation.

Takeshima et al. [TTFN05] utilized the *volume skeleton tree* to define topological attributes as additional input for specifying multidimensional transfer functions. Their settings of transfer functions are based on fixed topological indices, such as depth of topological nesting. Weber et al. [WDC*07] generalized the work of Takeshima et al. [TTFN05] by allowing the user to assign independent transfer functions to topologically distinct features. These features do not need to share the same topological indices. They segmented a volume into regions where each region corresponds to a branch of a hierarchical contour tree decomposition, and applied a separate transfer function to each region.

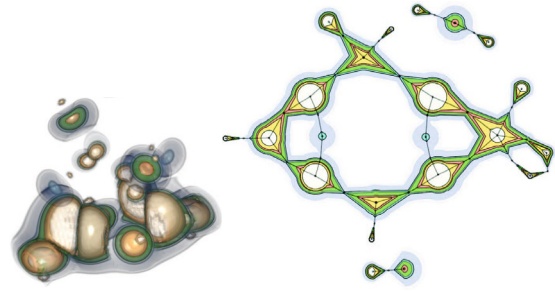


Figure 15: The topological spine of the neghip data set. The spine preserves the symmetry and cyclic structure of the molecule. Images © 2011 IEEE. Reprinted with kind permission from Correa et al. [CLB11] and IEEE.

Zhou and Takatsuka [ZT09] used the contour tree as a visual index to volume segments and utilized topological attributes for automatic transfer function specification. They employed the opacity residue flow model to contour tree branches and provided user interfaces for generating the transfer function.

Weber et al. [WBP07] introduced the *topological landscape*, a 2D terrain with the same topology as a given high-dimensional data set for easy understanding the topological structure. They first extracted the contour tree from a scalar function, then constructed its branch decomposition [PCMS05], and finally recursively created a terrain with the same topological structure as the original data. The topological landscape also preserves the persistence and volume of each feature. It provides a powerful interface to complement existing contour tree based techniques. Figure 14 shows an example of topological landscape. Based on the topological landscape metaphor, Harvey and Wang [HW10] presented *topological landscape ensembles*, a collection of 2D terrain models which preserves the contour tree of the input high-dimensional scalar field. They leveraged the treemap layout [Shn92] to construct the terrain layout and provided a simple interface for users to explore the terrain model.

4.2. Neighborhood Graphs

Neighborhood graphs connect points based on their proximity information to create a geometric structure of the data. Well-known examples of neighborhood graphs include the *k-NN graph*, *relative neighborhood graph* [JT92], and *Delauray triangulation*.

Bremer et al. [BPH05] presented the *cancellation tree* which simplifies a Morse-Smale complex of a function's topology by successively canceling pairs of critical points. Through effective encoding the cancellations, they produced an adaptive topology-based multiresolution representation of the function. This leads to a concise subset of the Morse-Smale complex that connects maxima or minima in a tree.

Correa et al. [CLB11] introduced *topological spines*, a vi-

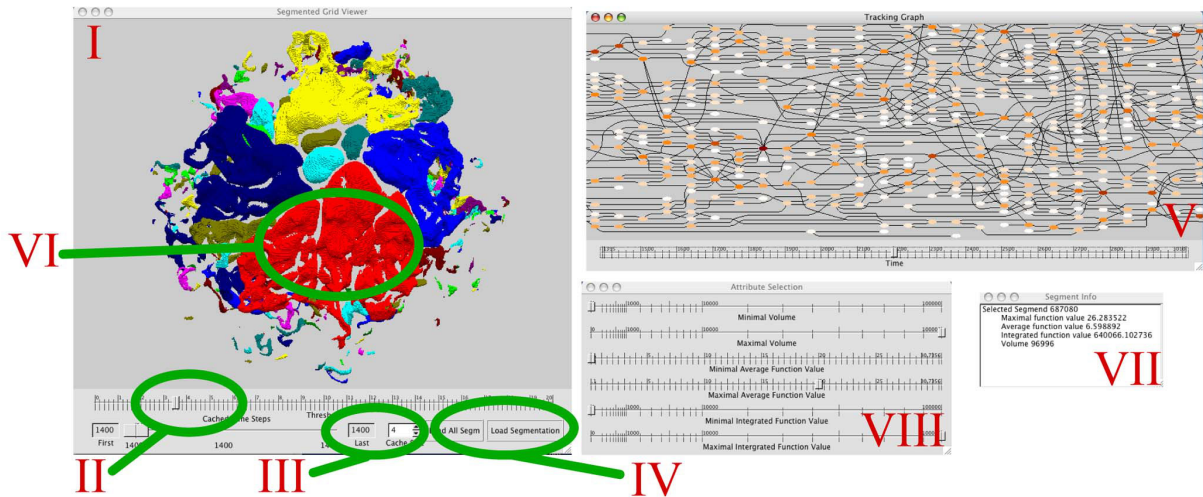


Figure 16: (I) 3D display of the segmentation of burning cells from the turbulent combustion data set with various interface controls (II to IV). (V) interactive display of the tracking graph. A selected node is highlighted in (VI) and its attribute information is displayed in (VII). (VIII) is for subsection of segments based on attribute values. Image © 2011 IEEE. Reprinted with kind permission from Bremer et al. [BWT*11] and IEEE.

visual representation that preserves both topological and structural properties of a scalar field. Topological spines are based on *extremum graphs* that describe the connectivity of the spine by connecting critical points along steepest ascending (or descending) lines. Topological spines are enhanced visual representations of extremum graphs with geometric and contour nesting information. They not only abstract the shape and structure of complex 3D scalar data, but also present 2D maps to facilitate feature selection and tracking. As shown in Figure 15, compared with other representations such as the contour tree and Morse-Smale complex, topological spines are better suited for spatial reasoning due to the preservation of the topology and locality of extrema and the nesting structure of the surrounding contours.

Correa and Lindström [CL11] studied the *empty region graphs* (ERGs) to improve the robustness of neighborhood-based analysis methods. In an ERG, two points are connected if a canonical region around them does not contain any other point. Examples of ERGs are the *nearest neighbor graph*, *relative neighborhood graph*, *Gabriel graph*, *diamond graph*, and β -*skeletons* [CL11]. They generalized ERGs to natural ERGs (which guarantee certain neighborhood and space partitioning properties), relaxed ERGs (a variation which is less sensitive to the sparsity and distribution of samples), and stochastic ERGs (a generalization that introduces the likelihood of samples being neighbors).

4.3. Topological Feature Tracking

Soho and Bajaj [SB06] applied the contour tree for time-varying contour tracking. They first constructed the contour tree at every time step and computed the correspondence in-

formation among contour trees across time steps given an isovalue. The *topology change graph* is constructed by creating a node for every intersection point and connecting each pair of intersection points where their representative contours correspond to each other. This graph allows detection of significant topological and geometric changes in time-varying isosurfaces. It also serves as an interface for users to segment, track and visualize the evolution of selected contour components over time.

Bremer et al. [BWT*11] constructed a *hierarchical merge tree* for each time step with augmented attributes using a streaming algorithm and then created tracking graphs to capture the temporal evolution of features. As shown in Figure 16, a linked-view interface is provided to explore the time evolution of the graph along with segmented data features. Widanagamaachchi et al. [WCB12] built a compact *meta-graph* to store the sequence of feature families and to encode all possible tracking graphs and relevant attributes. At run time, they interactively extracted, filtered and simplified a *dynamic tracking graph* from the meta-graph to explore the temporal evolution of features. The tracking graph also provides a user interface that is integrated into the 3D view of current feature sets for brushing and linking.

For multivariate feature tracking, Bennett et al. [BKL*11] encoded the set of all possible flow features by pre-computing merge trees augmented with attributes. The resulting multiresolution feature hierarchy enables flexible and interactive feature analysis, allowing the exploration of the entire feature family without accessing the original data. McLendon et al. [MBB*12] developed an *attributed relational graph* (ARG) to capture the structural relationships

defined by multiple variables. In the ARG, nodes represent features defined by an arbitrary number of variables, and edges encode the relationship between these features both within and across time steps. They presented a query-based search interface for users to identify events of interest characterized by subgraph-isomorphism search heuristics.

4.4. Symmetry Detection and Structure Comparison

Thomas and Natarajan [TN11, TN13] studied the symmetry in scalar field topology. *Symmetry* in scalar fields refers to different parts of the data that are invariant in the scalar field distribution. In [TN11], they analyzed the topology of level sets in a scalar field using the contour tree to detect symmetric patterns. With a similarity measure for comparing subtrees, they identified subtrees in the contour tree that are similar for grouping and extracted regions corresponding to a common group as symmetric components. In [TN13], they presented the *augmented extremum graph* and designed a symmetry detection algorithm based on robust distance estimation. The augmented extremum graph is based on the extremum graph [CLB11]. It captures both topological and geometric information of the scalar field and enables computationally efficient detection of symmetry. This method improves the previous work [TN11] in that it is aware of the underlying geometry and can detect global symmetry even in the presence of significant noise.

Schneider et al. [SWC*08] presented a solution for interactive comparison of scalar fields using isosurfaces. They defined features as the largest contour segmentation after topological simplification and compared features based on their spatial overlap. They designed the *similarity browser* to show the similarities between features and used the contour trees for navigation. They also combined the contour tree with the λ_2 algorithm to detect and compare features in fluid-flow related scalar fields. Saikia et al. [SSW14] studied the topological structures defined by their sub-level or super-level sets for identifying repeating structures. They introduced the *extended branch decomposition graph* (eBDG) which represents a forest of *branch decomposition trees* (BDTs) [PCMS05] where each of the BDTs is computed from a subtree of the merge tree. The eBDG is leveraged to finding similar structures in the same data set, detecting periodic patterns in different time steps, and comparing the topology in different data sets.

Chan et al. [CQC*08] presented a relation-aware pipeline for volume exploration. They employed region connection calculus (RCC) to define relations between structures in a volume and represented these relations as a *relation graph* for understanding and navigation. In their relation graph, nodes represent segments (i.e., homogenous regions) and links represent the spatial relations between segments. Unlike the contour tree which focuses on the nesting relations of isosurfaces, the relation graph focuses on structure segments and considers a more complete set of spatial relations (separate, touch, overlap and enclose).

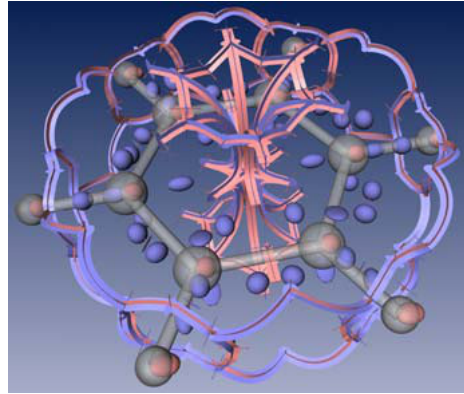


Figure 17: Visualization of the topological skeleton along with saddle connectors. A double flow ribbon approach is applied to visualize the orientation of the separation surfaces in the neighborhood of the saddle connector. Image © 2003 IEEE. Reprinted with kind permission from Theisel et al. [TWH03] and IEEE.

4.5. Vector Field Topology

Topological analysis of vector fields is based on the critical points and their connections through integration of special streamlines called *separatrices* [HH89]. The resulting topological skeletons enable users to visually comprehend the structure of the vector field by partitioning the domain into subregions of uniform flow behaviors.

Visualization of the topological skeleton of a 3D vector field requires simultaneous display of a large number of streamsurfaces, which easily leads to visual clutter. To address this issue, Theisel et al. [TWH03] presented *saddle connectors* that create sparse visual representations by representing separation surfaces as a finite number of streamlines. These streamlines are the intersection curves of separation surfaces, and start and end in saddle points. Figure 17 shows an example of the topological skeleton with saddle connectors.

Based on Morse decompositions, Chen et al. [CML*07] presented the *Morse connection graphs* (MCGs) and their refinement *entity connection graphs* (ECGs) to extract and visualize boundary flow topology on surfaces. MCG augments the vector field skeleton by addressing *periodic orbits*. Szymczak and Sipeki [SS13] presented an algorithm for drawing the MCG for topologically rich vector fields. The proposed visual representation of the MCG preserves the spatial relationships between its arcs and nodes and highlights the coherence between connecting trajectories.

The *transition graph* [SZ12] and *super-transition graph* [Szy11] have been proposed for robust and stable Morse decompositions for piecewise constant vector fields. The difference between these two graphs is that a transition graph represents trajectories of a single piecewise linear vector

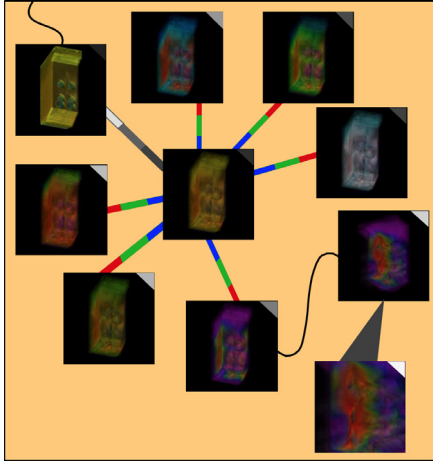


Figure 18: Image graph for exploring the furnace data set. The user first searches for an appropriate color transfer function before deriving the desirable visualization shown in the lower right image. Image © 1999 IEEE. Reprinted with kind permission from Ma [Ma99] and IEEE.

field, while a super-transition graph represents trajectories of all feasible vector fields.

4.6. Multifield Topology

Compared with univariate scalar field topology, much less work has been done on topological analysis and visualization of multivariate scalar fields. Carr and Duke [CD14] introduced *joint contour nets* (JCNs) which generalize the contour tree analysis for univariate scalar fields to multifields. The JCN is an approximation of the Reeb space of an arbitrary number of variables. The quantized contour trees of the single fields can be extracted from the JCN using a quotient graph algorithm. Huettenberger et al. [HHC*13] extended the topological structures from single scalar field to multifields using the concepts of Pareto optimality and Pareto dominance. For multivariate point clouds, Riech et al. [RL14] introduced the *simplicial chain graphs* as a visual metaphor of the inhomogeneous topological structure. They calculated the persistent homology of the data set and derived a localized description of simplicial chains, from which a graph structure was created to obtain the structural information.

5. Provenance-wise Representations and Techniques

Provenance refers to the lineage of an item. In the context of scientific workflow, it refers to all the information necessary to reproduce a certain piece of data. Although not a great deal of work relating to provenance- or history-wise graph representations and techniques has been done, this direction of research has its distinct foci and unique purposes. It dates back to the concept of “visualizing visualizations” [Ma00] which aims at better managing and exploring visualization

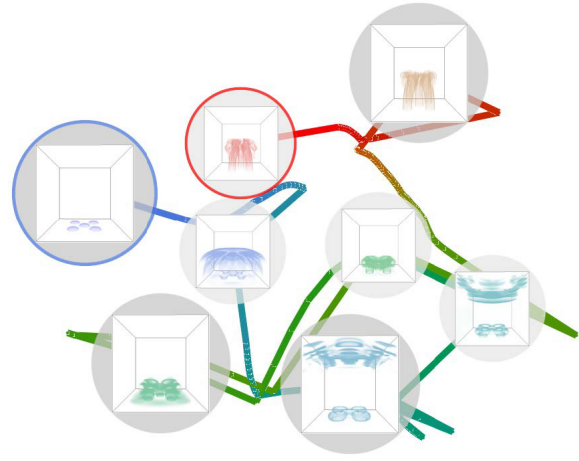


Figure 19: A storyboard of the time-varying five jets data set. Blue to green to red are for early to middle to later time steps. Image © 2008 IEEE. Reprinted with kind permission from Lu and Shen [LS08] and IEEE.

processes and results. Later works extended this idea to storytelling generation, animation creation, and simulation parameter space exploration. For provenance visualization, the graphs produced resemble flowcharts widely used in designing and documenting complex processes or programs.

5.1. Visualizing Visualizations

The process of visual data exploration contains a wealth of information: parameters, results, history, as well as relationships among them. To learn lessons and share experiences, the process itself can be stored, tracked and analyzed. It can also be incorporated into, and thus becomes a part of the user interface of a visualization system. The work of *image graphs* by Ma [Ma99] was the first that visualizes the visualization process. As shown in Figure 18, image graphs represent not only the results but also the process of data visualization. Each node in an image graph records an image and the corresponding visualization parameters used to produce it. Each edge in the graph shows the change in rendering parameters (e.g., color, opacity, rotation, zoom, shading, sampling, etc.) between the two nodes it connects.

Jankun-Kelly and Ma [JKM01] introduced a *spreadsheet-like interface* for visualization exploration. The interface displays the visualization parameter space and presents a clear correspondence between parameters and results through tabular organization. Jankun-Kelly et al. [JKMG02] further formalized a general model of the visualization exploration process. They designed the *derivation graph*, a collection of directed acyclic graphs to represent relationships between parameter value derivations. Each node in the graph represents a single session result. A directed edge exists between two nodes if and only if the node with the outgoing edge derives the node with the incoming edge.

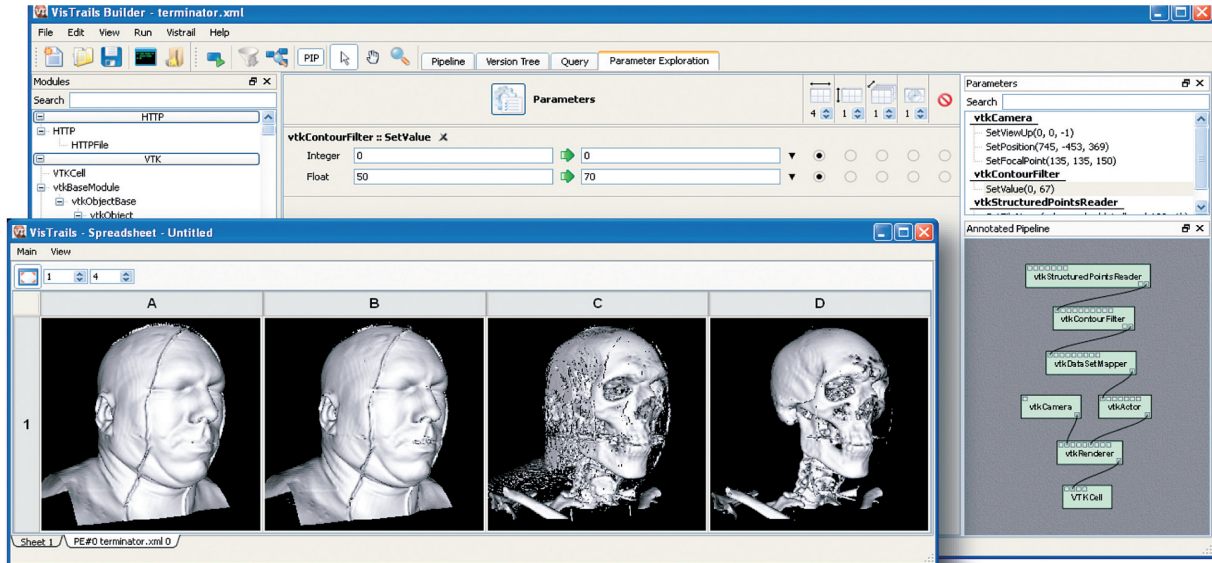


Figure 20: The VisTrails builder and spreadsheet show the dataflow and visualization products. Image © 2007 IEEE. Reprinted with kind permission from Silva et al. [SFC07] and IEEE.

Woodring and Shen [WS06b] proposed a volume shader for users to easily select and operate on many data volumes to create comparative visualization. They showed the contextual visualization of the volume shader by converting it to a *volume tree*. In a volume tree, nodes are operators and input data fields, and edges are input and output connections between operators. The visualization result is the root, and all input fields are leaves. One operational step forward in forming the final result is indicated by one level of the tree. The context is defined as the suboperations (i.e., subtrees of the volume tree) that form the final result.

5.2. Storytelling, Animation and Simulation

Storytelling provides a powerful means for exploration and communication of data. Ma et al. [MLF*12] referred to *scientific storytelling* as telling stories using scientific data. Wohlfart and Hauser [WH07] introduced a *story model* that includes story nodes and story transitions. Story nodes are major steps or milestones in which a story briefly halts (for interactive exploration by the story consumer, for example) and then resumes. Story transitions connect story nodes smoothly leading from one node to the next.

Lu and Shen [LS08] presented an *interactive storyboard* for time-varying data visualization. As shown in Figure 19, the storyboard displays sample images and line drawings in a clear 2D layout to summarize complex data dynamics, such as relevancies and differences, in a concise and effective manner. Yu et al. [YLRC10] designed an *event graph* for automatic animation of time-varying data. The event graph embeds a tree-like structure and includes nodes, tree links, and relation links. Nodes represent event features from sev-

eral aspects and at different scales. Tree links indicate the child and parent relationships of nodes belonging to the same feature aspect. Relation links indicate the similarities of time durations of nodes from different feature aspects. Balabanian et al. [BVG10] explored the combination of hierarchical data space and 3D spatial space. The input volumetric data set is segmented and hierarchically organized. They utilized a tree as a guiding structure for visual exploration of relationships among segmented components. The spatial characteristics of the data were integrated within the abstract view.

Timelines are commonly used in animation control and parameter exploration. Related work in this direction includes the timeline-based mixer (including multiple tracks and a template chooser) for creating animations for volume visualization [AWM10] and the timeline-based graph for exploring simulation parameter space [BM10].

5.3. Provenance Visualization

Typical visualization solutions only require final results. Besides final results, provenance visualization also includes capabilities for visualizing intermediate or partial results, derivation processes, and any information associated with used sources. Provenance techniques can facilitate the comprehension, verification and reproduction of scientific results by providing access to information about the sources and methods used to derive them.

The most notable example of provenance visualization is *VisTrails* [BCC*05, SFC07], a system that provides infrastructure for data exploration and visualization through workflows. An example of VisTrails builder and spreadsheet is

shown in Figure 20. Provenance information managed by VisTrails refers to the modifications (e.g., addition, deletion or replacement) or history of changes made to a particular workflow in order to derive a new workflow. VisTrails renders this history of modifications as a tree-like structure where nodes represent a version of some workflow and edges represent the modification applied to a workflow in order to derive a new workflow. Upon accessing a particular node of the *provenance tree*, users are provided with a rendering of the scientific product which is generated as a result of a particular workflow associated with the node. Due to the clear separation between the specification of a pipeline and its execution instances, VisTrails features powerful scripting capabilities and provides a scalable mechanism for generating a large number of visualizations.

Groth and Streefkerk [GS06] presented a conceptual interaction model to support provenance and annotation for visual exploration systems. In their *interaction graph*, nodes represent measurable states of the visualization system and edges denote transitions between states. States of the system are generically captured in the model and transitions might contain discrete interactions, such as zooming, translation, rotation, etc. Their model concisely captures state changes made by the user so that the recall of the steps taken to achieve the visual representation can be retrieved. By articulating with annotations, the prototypes implemented support a wide variety of knowledge discovery tasks as well as collaborative discovery and recall of past explorations.

6. Research Trends

Throughout this survey, we have observed several research trends in graph-based representations and techniques for scientific visualization:

From Internal to External Representations. Early work on tree and graph structures focused on data representation and organization, mainly for adaptive processing and rendering. These representations were mostly internal, addressing issues such as data reduction and reuse, memory and I/O efficiency, and rendering performance. Over the years, these representations have gradually shifted from internal to external. Most external representations display the graph in a separate 2D view to avoid occlusion rather than superimposing the graph in the original 3D spatial data view. These external representations go beyond the traditional boundary of scientific visualization and incorporate information visualization techniques toward effective analysis of scientific data. Besides showing an overview of the data and relationships as abstract visual graphs, they also serve as interfaces for user interaction. In conjunction with the original data view via brushing and linking, users are able to compare relationships, track changes, and gain a more complete view and flexible control over data navigation and exploration.

From Simple to Complex Graphs. Graph representations are moving from simple to complex, small to large, often with hierarchical, sometime compound structures. This

is partly because the research in scientific visualization has moved from univariate to multivariate data, from scalar to vector fields, and from steady to unsteady data. As the data get larger and more complicated, the corresponding graphs need to consider more advanced forms to encode various data relationships. Another reason that contributes to this trend lies in the growing need to tackle big data with coarse-to-fine analysis capability. Such a graph representation should allow users to not only gain a quick global overview but also identify local features and patterns, in a way that should be more simpler and easier to achieve in the transformed graph view than in the original data view.

From Straightforward to Advanced Solutions. As graphs derived from scientific data sets get larger and more complex, more advanced graph techniques from information visualization and graph drawing have been applied for effective visualization and interaction. From simple fixed graph layouts such as circular layouts to flexible force-directed layouts, from straightforward graph visualization to advanced spectral layout and layered graphs, from single graph to hierarchical and compound graph drawing, from steady to dynamic graphs, this trend will remain active and we expect more applications of state-of-the-art graph visualization techniques to investigate scientific data sets. We also expect novel graph interaction and navigation solutions to be presented in order to handle the ever-growing graphs in terms of both size and complexity.

7. Remaining Challenges

Remaining challenges for graph-based representations and techniques in scientific visualization include the following:

Graph Simplification and Mining. As the graphs derived from scientific data sets get larger and more complex, there is a pressing need to process and present the graphs in a simplified form for easy human understanding and navigation. Techniques such as graph simplification will be very helpful to reduce the workload, both visually and manually, of users toward cost-effective analysis. When the data set is large and the relationships are complex, it might be simply impossible for users to find out community structures and track features over time in the resulting graph. Graph mining solutions could automatically identify communities and hotspots for detecting trends and anomalies, and align multiple graphs or subgraphs for finding common features and distinct patterns. These solutions will be more efficient and effective than simply asking users to extract relationships via standard brushing and linking techniques. Such graph functions represent a significant step forward and will be in great demand for big data visualization.

Online Streaming and In-Situ Graphs. Most current graph algorithms and techniques presented for scientific visualization, especially for those presented in a visual form for navigation and interaction, are built offline and on a single machine. Solutions for streaming, parallel and in-situ

scenarios have not been explored. To fully leverage the aggregated computing power, we need to not only develop online dynamic graph solutions for extreme-scale scientific data but also incorporate graph generation, visualization and interaction into parallel and in-situ visualization. Much work remains to be done in order to demonstrate the feasibility, capability and scalability of graph-based techniques for analyzing and visualizing scientific data sets of terabytes, petabytes and beyond.

Evaluation and Knowledge Discovery. Since graphs are abstract representations extracted from scientific data sets, it is imperative to show that the added graph view would not increase much the burden for users to understand the underlying data but rather facilitate such a process. Early work on graph-based representations and techniques seldom included user evaluation. Recent work that presented visual graphs for navigation and exploration often incorporated ad-hoc feedback from domain experts or scientists. More rigorous evaluations are needed in order to verify that graph-based solutions indeed help scientists in their visual analysis and discovery of knowledge previously unknown or unable to get without the graphs. As transformation-based solutions for scientific visualization get increasingly popular, formal evaluation of general graph-based techniques for scientific visualization becomes necessary. This evaluation presents quite a few challenges ranging from evaluation design, experiment to analysis as many current solutions are restricted to one kind of scientific data or even tied together with a particular scientific application. Nevertheless, existing guidelines and practices for graph evaluation from information visualization offer practical guidance to achieve this goal.

8. Conclusions

We have presented a survey of graph-based representations and techniques for scientific visualization. The survey reviews related work in four categories and points out research trends and remaining challenges. A notable trend in this research is to develop graph-based visual representations and interfaces for scientific visualization, targeting large-scale time-varying multivariate scalar and vector field data. We believe that this direction of research is still on the rise as a number of new graph mappings and interactions have been introduced recently.

Many challenges remain to be solved which are related to big scientific data visualization. Novel graph-based solutions for streaming, parallel and in-situ settings are in great demand. The evaluation of graph-based techniques for scientific visualization is only in its infancy and much remains to be explored. We believe that the success of graph-based techniques will fundamentally change the tools and feature sets we have at hand to perform scientific visualization on a regular basis. Eventually, such graph views would become commonplace for researchers and vendors to integrate and provide in the scientific visualization workflow.

Acknowledgements

This work was supported in part by the U.S. National Science Foundation through grants IIS-1456763 and IIS-1455886. The author would like to thank Yi Gu for helping the identification of related publications.

References

- [AWM10] AKIBA H., WANG C., MA K.-L.: AniViz: A template-based animation tool for volume visualization. *IEEE Computer Graphics and Applications* 30, 5 (2010), 61–71. [15](#)
- [BAAK*13] BEYER J., AL-AWAMI A., KASTHURI N., LICHTMAN J. W., PFISTER H., HADWIGER M.: ConnectomeExplorer: Query-guided visual analysis of large volumetric neuroscience data. *IEEE Transactions on Visualization and Computer Graphics* 19, 12 (2013), 2868–2877. [8](#)
- [BBDW14] BECK F., BURCH M., DIEHL S., WEISKOPF D.: The state of the art in visualizing dynamic graphs. In *Eurographics Conference on Visualization - State-of-the-Art Reports* (2014). [3](#)
- [BCC*05] BAVOIL L., CALLAHAN S. P., CROSSNO P. J., FREIRE J., SCHEIDEGGER C. E., SILVA C. T., VO H. T.: Vis-Trails: Enabling interactive multiple-view visualizations. In *Proceedings of IEEE Visualization Conference* (2005), pp. 135–142. [15](#)
- [BDSW13] BISWAS A., DUTTA S., SHEN H.-W., WOODRING J.: An information-aware framework for exploring multivariate data sets. *IEEE Transactions on Visualization and Computer Graphics* 19, 12 (2013), 2683–2692. [7](#)
- [BKL*11] BENNETT J. C., KRISHNAMOORTHY V., LIU S., GROUT R. W., HAWKES E. R., CHEN J. H., SHEPHERD J., PASCUCCI V., BREMER P.-T.: Feature-based statistical analysis of combustion simulation data. *IEEE Transactions on Visualization and Computer Graphics* 17, 12 (2011), 1822–1831. [12](#)
- [BM10] BRUCKNER S., MÖLLER T.: Result-driven exploration of simulation parameter spaces for visual effects design. *IEEE Transactions on Visualization and Computer Graphics* 16, 6 (2010), 1468–1476. [15](#)
- [BNS01] BOADA I., NAVAZO I., SCOPIGNO R.: Multiresolution volume visualization with a texture-based octree. *The Visual Computer* 17, 3 (2001), 185–197. [4](#)
- [BPH05] BREMER P.-T., PASCUCCI V., HAMANN B.: Maximizing adaptivity in hierarchical topological models. In *Proceedings of International Conference on Shape Modeling and Applications* (2005), pp. 298–307. [11](#)
- [BPS97] BAJAJ C. L., PASCUCCI V., SCHIKORE D. R.: The contour spectrum. In *Proceedings of IEEE Visualization Conference* (1997), pp. 167–173. [10](#)
- [BSL*14] BÖTTGER J., SCHÄFER A., LOHMANN G., VILLRINGER A., MARGULIES D. S.: Three-dimensional mean-shift edge bundling for the visualization of functional connectivity in the brain. *IEEE Transactions on Visualization and Computer Graphics* 20, 3 (2014), 471–480. [8](#)
- [BVG10] BALABANIAN J.-P., VIOLA I., GRÖLLER M. E.: Interactive illustrative visualization of hierarchical volume data. In *Proceedings of Graphics Interface* (2010), pp. 137–144. [15](#)
- [BWT*11] BREMER P.-T., WEBER G., TIERNY J., PASCUCCI V., DAY M., BELL J.: Interactive exploration and analysis of large-scale simulations using topology-based data segmentation. *IEEE Transactions on Visualization and Computer Graphics* 17, 9 (2011), 1307–1324. [12](#)

- [Car04] CARR H.: *Topological Manipulation of Isosurfaces*. PhD thesis, The University of British Columbia, 2004. 10
- [CD14] CARR H., DUKE D.: Joint contour nets. *IEEE Transactions on Visualization and Computer Graphics* 20, 8 (2014), 1100–1113. 14
- [CF11] CARMONA R., FROEHLICH B.: Error-controlled real-time cut updates for multi-resolution volume rendering. *Computers & Graphics* 35, 4 (2011), 931–944. 4
- [CL11] CORREA C. D., LINDSTRÖM P.: Towards robust topology of sparsely sampled data. *IEEE Transactions on Visualization and Computer Graphics* 17, 12 (2011), 1852–1861. 12
- [CLB11] CORREA C. D., LINDSTRÖM P., BREMER P.-T.: Topological spines: A structure-preserving visual representation of scalar fields. *IEEE Transactions on Visualization and Computer Graphics* 17, 12 (2011), 1842–1851. 11, 13
- [CML*07] CHEN G., MISCHAIKOW K., LARAMEE R. S., PILARCZYK P., ZHANG E.: Vector field editing and periodic orbit extraction using Morse decomposition. *IEEE Transactions on Visualization and Computer Graphics* 13, 4 (2007), 769–785. 13
- [CNLS12] CHEN C.-M., NOUANESSENGSY B., LEE T.-Y., SHEN H.-W.: Flow-guided file layout for out-of-core pathline computation. In *Proceedings of IEEE Symposium on Large Data Analysis and Visualization* (2012), pp. 109–112. 9
- [CQC*08] CHAN M.-Y., QU H., CHUNG K.-K., MAK W.-H., WU Y.: Relation-aware volume exploration pipeline. *IEEE Transactions on Visualization and Computer Graphics* 14, 6 (2008), 1683–1690. 13
- [CS13] CHEN C.-M., SHEN H.-W.: Graph-based seed scheduling for out-of-core FTLE and pathline computation. In *Proceedings of IEEE Symposium on Large Data Analysis and Visualization* (2013), pp. 15–23. 9
- [CSA03] CARR H., SNOEYINK J., AXEN U.: Computing contour trees in all dimensions. *Computational Geometry: Theory and Applications* 24, 2 (2003), 75–94. 10
- [CSvdP04] CARR H., SNOEYINK J., VAN DE PANNE M.: Simplifying flexible isosurfaces using local geometric measures. In *Proceedings of IEEE Visualization Conference* (2004), pp. 497–504. 10, 11
- [CSvdP10] CARR H., SNOEYINK J., VAN DE PANNE M.: Flexible isosurfaces: Simplifying and displaying scalar topology using the contour tree. *Computational Geometry* 43, 1 (2010), 42–58. 11
- [CXLS12] CHEN C.-M., XU L., LEE T.-Y., SHEN H.-W.: A flow-guided file layout for out-of-core streamline computation. In *Proceedings of IEEE Pacific Visualization Symposium* (2012), pp. 145–152. 9
- [DCS09] DU Z., CHIANG Y.-J., SHEN H.-W.: Out-of-core volume rendering for time-varying fields using a space-partitioning time (SPT) tree. In *Proceedings of IEEE Pacific Visualization Symposium* (2009), pp. 73–80. 5
- [FJS96] FINKELSTEIN A., JACOBS C. E., SALESIN D. H.: Multiresolution video. In *Proceedings of ACM SIGGRAPH Conference* (1996), pp. 281–290. 5
- [GKHS98] GAGVANI N., KENCHAMMANA-HOSEKOTE D., SILVER D.: Volume animation using the skeleton tree. In *Proceedings of IEEE Symposium on Volume Visualization* (1998), pp. 47–53. 11
- [GRT14] GÜNTHER T., RÖSSL C., THEISEL H.: Hierarchical opacity optimization for sets of 3D line fields. *Computer Graphics Forum* 33, 2 (2014), 507–516. 6
- [GS06] GROTH D. P., STREEFKERK K.: Provenance and annotation for visual exploration systems. *IEEE Transactions on Visualization and Computer Graphics* 12, 6 (2006), 1500–1510. 16
- [GW11] GU Y., WANG C.: TransGraph: Hierarchical exploration of transition relationships in time-varying volumetric data. *IEEE Transactions on Visualization and Computer Graphics* 17, 12 (2011), 2015–2024. 7
- [GW13] GU Y., WANG C.: iTree: Exploring time-varying data using indexable tree. In *Proceedings of IEEE Pacific Visualization Symposium* (2013), pp. 137–144. 6
- [GWGS02] GUTHE S., WAND M., GONSER J., STRASSER W.: Interactive rendering of large volume data sets. In *Proceedings of IEEE Visualization Conference* (2002), pp. 53–60. 4
- [GWLS05] GAO J., WANG C., LI L., SHEN H.-W.: A parallel multiresolution volume rendering algorithm for large data visualization. *Parallel Computing* 31, 2 (2005), 185–204. 4
- [GY95] GHAVAMNIA M. H., YANG X. D.: Direct rendering of Laplacian pyramid compressed volume data. In *Proceedings of IEEE Visualization Conference* (1995), pp. 192–199. 4
- [HH89] HELMAN J. L., HESSELINK L.: Representation and display of vector field topology in fluid flow data sets. *IEEE Computer* 22, 8 (1989), 27–36. 13
- [HH*13] HUETTENBERGER L., HEINE C., CARR H., SCHEUERMANN G., GARTH C.: Towards multifield scalar topology based on pareto optimality. *Computer Graphics Forum* 32, 3 (2013), 341–350. 14
- [HMM00] HERMAN I., MELANCON G., MARSHALL M. S.: Graph visualization and navigation in information visualization: A survey. *IEEE Transactions on Visualization and Computer Graphics* 6, 1 (2000), 24–43. 3
- [HPSP01] HAHN H., PREIM B., SELLE D., PEITGEN H.-O.: Visualization and interaction techniques for the exploration of vascular structures. In *Proceedings of IEEE Visualization Conference* (2001), pp. 395–402. 10
- [HW10] HARVEY W., WANG Y.: Topological landscape ensembles for visualization of scalar-valued functions. *Computer Graphics Forum* 29, 3 (2010), 993–1002. 11
- [IVJ12] IP C. Y., VARSHNEY A., JAJA J.: Hierarchical exploration of volumes using multilevel segmentation of the intensity-gradient histograms. *IEEE Transactions on Visualization and Computer Graphics* 18, 12 (2012), 2355–2363. 6
- [JBS08] JÄNICKE H., BÖTTINGER M., SCHEUERMANN G.: Brushing of attribute clouds for the visualization of multivariate data. *IEEE Transactions on Visualization and Computer Graphics* 14, 6 (2008), 1459–1466. 6, 7
- [JKM01] JANKUN-KELLY T. J., MA K.-L.: Visualization exploration and encapsulation via a spreadsheet-like interface. *IEEE Transactions on Visualization and Computer Graphics* 7, 3 (2001), 275–287. 14
- [JKMG02] JANKUN-KELLY T., MA K.-L., GERTZ M.: A model for the visualization exploration process. In *Proceedings of IEEE Visualization Conference* (2002), pp. 323–330. 14
- [JS09] JÄNICKE H., SCHEUERMANN G.: Steady visualization of the dynamics in fluids using epsilon-machines. *Computers & Graphics* 33, 5 (2009), 597–606. 7
- [JT92] JAROMCZYK J. W., TOUSSAINT G. T.: Relative neighborhood graphs and their relatives. *Proceedings of the IEEE* 80, 9 (1992), 1502–1517. 11
- [Lev90] LEVOY M.: Efficient ray tracing of volume data. *ACM Transactions on Graphics* 9, 3 (1990), 245–261. 4

- [LH91] LAUR D., HANRAHAN P.: Hierarchical splatting: A progressive refinement algorithm for volume rendering. In *Proceedings of ACM SIGGRAPH Conference* (1991), pp. 285–288. 4
- [LHJ99] LAMAR E., HAMANN B., JOY K. I.: Multiresolution techniques for interactive texture-based volume visualization. In *Proceedings of IEEE Visualization Conference* (1999), pp. 355–362. 4
- [LLRR08] LINSEN L., LONG T. V., ROSENTHAL P., ROSSWOG S.: Surface extraction from multi-field particle volume data using multi-dimensional cluster visualization. *IEEE Transactions on Visualization and Computer Graphics* 14, 6 (2008), 1483–1490. 6
- [LPD*02] LINSEN L., PASCUCCI V., DUCHAINEAU M. A., HAMANN B., JOY K. I.: Hierarchical representation of time-varying volume data with $\sqrt[3]{2}$ subdivision and quadrilinear B-spline wavelets. In *Proceedings of Pacific Conference on Computer Graphics and Applications* (2002), pp. 346–355. 4
- [LS08] LU A., SHEN H.-W.: Interactive storyboard for overall time-varying data visualization. In *Proceedings of IEEE Pacific Visualization Symposium* (2008), pp. 143–150. 14, 15
- [Ma99] MA K.-L.: Image graphs - a novel approach to visual data exploration. In *Proceedings of IEEE Visualization Conference* (1999), pp. 81–88. 14
- [Ma00] MA K.-L.: Visualizing visualizations: User interfaces for managing and exploring scientific visualization data. *IEEE Computer Graphics and Applications* 20, 5 (2000), 16–19. 14
- [MBB*12] MCLENDON W. C., BANSAL G., BREMER P.-T., CHEN J., KOLLA H., BENNETT J. C.: On the use of graph search techniques for the analysis of extreme-scale combustion simulation data. In *Proceedings of IEEE Symposium on Large-Scale Data Analysis and Visualization* (2012), pp. 57–63. 12
- [Mea82] MEAGHER D. J.: Geometric modeling using octree encoding. *Computer Graphics and Image Processing* 19, 2 (1982), 129–147. 4
- [MLF*12] MA K.-L., LIAO I., FRAZIER J., HAUSER H., KOSTIS H.-N.: Scientific storytelling using visualization. *IEEE Computer Graphics and Applications* 32, 1 (2012), 12–19. 15
- [MPH94] MA K.-L., PAINTER J. S., HANSEN C. D.: Parallel volume rendering using binary-swap compositing. *IEEE Computer Graphics and Applications* 14, 4 (1994), 59–67. 5
- [MS00] MA K.-L., SHEN H.-W.: Compression and accelerated rendering of time-varying data. In *Proceedings of International Computer Symposium - Workshop on Computer Graphics and Virtual Reality* (2000), pp. 82–89. 4
- [MWS13] MA J., WANG C., SHENE C.-K.: FlowGraph: A compound hierarchical graph for flow field exploration. In *Proceedings of IEEE Pacific Visualization Symposium* (2013), pp. 233–240. 7, 8
- [MWSJ14] MA J., WANG C., SHENE C.-K., JIANG J.: A graph-based interface for visual analytics of 3D streamlines and pathlines. *IEEE Transactions on Visualization and Computer Graphics* 20, 8 (2014), 1127–1140. 4, 8
- [NLS11] NOUANESNGSY B., LEE T.-Y., SHEN H.-W.: Load-balanced parallel streamline generation on large scale vector fields. *IEEE Transactions on Visualization and Computer Graphics* 17, 12 (2011), 1785–1794. 9
- [OFH*11] OELTZE S., FREILER W., HILLERT R., DOLEISCH H., PREIM B., SCHUBERT W.: Interactive, graph-based visual analysis of high-dimensional, multi-parameter fluorescence microscopy data in toponomics. *IEEE Transactions on Visualization and Computer Graphics* 17, 12 (2011), 1882–1891. 7
- [OSBM14] OZER S., SILVER D., BEMIS K., MARTIN P.: Activity detection in scientific visualization. *IEEE Transactions on Visualization and Computer Graphics* 20, 3 (2014), 337–390. 9
- [PCMS05] PASCUCCI V., COLE-MCLAUGHLIN K., SCORZELLI G.: *Multi-Resolution Computation and Presentation of Contour Trees*. Tech. Rep. UCRL-PROC-208680, Lawrence Livermore National Laboratory, 2005. 11, 13
- [PO08] PREIM B., OELTZE S.: 3D visualization of vasculature: An overview. In *Visualization in Medicine and Life Sciences, Mathematics and Visualization*. Springer Berlin Heidelberg, 2008, pp. 39–59. 10
- [QCX*07] QU H., CHAN W.-Y., XU A., CHUNG K.-L., LAU K.-H., GUO P.: Visual analysis of the air pollution problem in Hong Kong. *IEEE Transactions on Visualization and Computer Graphics* 13, 6 (2007), 1408–1415. 7
- [RL14] RIECH B., LEITTE H.: Structural analysis of multivariate point clouds using simplicial chains. *Computer Graphics Forum* 33, 8 (2014), 28–37. 14
- [SB06] SOHN B.-S., BAJAJ C. L.: Time-varying contour topology. *IEEE Transactions on Visualization and Computer Graphics* 12, 1 (2006), 14–25. 12
- [SCM99] SHEN H.-W., CHIANG L.-J., MA K.-L.: A fast volume rendering algorithm for time-varying fields using a time-space partitioning (TSP) tree. In *Proceedings of IEEE Visualization Conference* (1999), pp. 371–377. 4
- [SFC07] SILVA C. T., FREIRE J., CALLAHAN S. P.: Provenance for visualizations: Reproducibility and beyond. *IEEE Computing in Science & Engineering* 9, 5 (2007), 82–89. 15
- [She98] SHEN H.-W.: Isosurface extraction in time-varying fields using a temporal hierarchical index tree. In *Proceedings of IEEE Visualization Conference* (1998), pp. 159–166. 4
- [Shn92] SHNEIDERMAN B.: Tree visualization with tree-maps: A 2D space-filling approach. *ACM Transactions on Graphics* 11, 1 (1992), 92–99. 5, 11
- [SIGM*11] SUTER S. K., IGLESIAS GUITIÁN J. A., MARTON F., AGUS M., ELSENER A., ZOLLIKOFER C. P. E., GOPI M., GOBBETTI E., PAJAROLA R.: Interactive multiscale tensor reconstruction for multiresolution volume visualization. *IEEE Transactions on Visualization and Computer Graphics* 17, 12 (2011), 2135–2143. 4
- [SMP13] SUTER S. K., MAKHYNIA M., PAJAROLA R.: TAM-RESH - tensor approximation multiresolution hierarchy for interactive volume visualization. *Computer Graphics Forum* 32, 3 (2013), 151–160. 4
- [SS13] SZYMCAK A., SIPEKI L.: Visualization of Morse connection graphs for topologically rich 2D vector fields. *IEEE Transactions on Visualization and Computer Graphics* 19, 12 (2013), 2763–2772. 13
- [SSW14] SAIKIA H., SEIDEL H.-P., WEINKAUF T.: Extended branch decomposition graphs: Structural comparison of scalar data. *Computer Graphics Forum* 33, 3 (2014), 41–50. 13
- [SSZC94] SAMTANEY R., SILVER D., ZABUSKY N., CAO J.: Visualizing features and tracking their evolution. *IEEE Computer* 27, 7 (1994), 20–27. 8
- [STS06] SAUBER N., THEISEL H., SEIDEL H.-P.: Multifield-Graphs: An approach to visualizing correlations in multifield scalar data. *IEEE Transactions on Visualization and Computer Graphics* 12, 5 (2006), 917–924. 7
- [SW97] SILVER D., WANG X.: Tracking and visualizing turbulent 3D features. *IEEE Transactions on Visualization and Computer Graphics* 3, 2 (1997), 129–141. 8

- [SWC*08] SCHNEIDER D., WIEBEL A., CARR H., HLA-
WITSCHKA M., SCHEUERMANN G.: Interactive comparison of
scalar fields based on largest contours with applications to flow
visualization. *IEEE Transactions on Visualization and Computer
Graphics* 14, 6 (2008), 1475–1482. 13
- [SZ12] SZYMCAK A., ZHANG E.: Robust Morse decomposi-
tions of piecewise constant vector fields. *IEEE Transactions on
Visualization and Computer Graphics* 18, 6 (2012), 851–860. 13
- [Szy11] SZYMCAK A.: Stable Morse decompositions for piece-
wise constant vector fields on surfaces. *Computer Graphics For-
um* 30, 3 (2011), 851–860. 13
- [TN11] THOMAS D. M., NATARAJAN V.: Symmetry in scalar
field topology. *IEEE Transactions on Visualization and Com-
puter Graphics* 17, 12 (2011), 2035–2044. 13
- [TN13] THOMAS D. M., NATARAJAN V.: Detecting symmetry
in scalar fields using augmented extremum graphs. *IEEE Trans-
actions on Visualization and Computer Graphics* 19, 12 (2013),
2663–2672. 13
- [TTFN05] TAKESHIMA Y., TAKAHASHI S., FUJISHIRO I.,
NIELSON G. M.: Introducing topological attributes for
objective-based visualization of simulated datasets. In *Pro-
ceedings of International Workshop on Volume Graphics* (2005),
pp. 137–236. 11
- [TWH03] THEISEL H., WEINKAUF T., HEGE H.-C., SEIDEL
H.-P.: Saddle connectors - an approach to visualizing the topol-
ogical skeleton of complex 3D vector fields. In *Proceedings of
IEEE Visualization Conference* (2003), pp. 225–232. 13
- [VLKS*11] VON LANDEBERGER T., KUIJPER A., SCHRECK
T., KOHLHAMMER J., VAN WIJK J. J., FEKETE J.-D., FELL-
NER D. W.: Visual analysis of large graphs: State-of-the-art
and future research challenges. *Computer Graphics Forum* 30,
6 (2011), 1719–1749. 3
- [WBP07] WEBER G. H., BREMER P.-T., PASCUCCI V.: Topo-
logical landscapes: A terrain metaphor for scientific data. *IEEE
Transactions on Visualization and Computer Graphics* 13, 6
(2007), 1416–1423. 11
- [WCB12] WIDANAGAMAACHCHI W., CHRISTENSENT C.,
BREMER P.-T.: Interactive exploration of large-scale time-
varying data using dynamic tracking graphs. In *Proceedings of
IEEE Symposium on Large Data Analysis and Visualization*
(2012), pp. 9–17. 12
- [WDC*07] WEBER G. H., DILLARD S. E., CARR H., PAS-
CUCCI V., HAMANN B.: Topology-controlled volume rendering.
IEEE Transactions on Visualization and Computer Graphics 13,
2 (2007), 330–341. 11
- [WH07] WOHLFART M., HAUSER H.: Story telling for presenta-
tion in volume visualization. In *Proceedings of Joint Eurograph-
ics - IEEE VGTC Symposium on Visualization* (2007), pp. 91–98.
15
- [WS04] WANG C., SHEN H.-W.: *A Framework for Rendering
Large Time-Varying Data Using Wavelet-Based Time-Space Par-
titioning (WTSP) Tree*. Tech. Rep. OSU-CISRC-1/04-TR05, The
Ohio State University, 2004. 5
- [WS05] WANG C., SHEN H.-W.: Hierarchical navigation inter-
face: Leveraging multiple coordinated views for level-of-detail
multiresolution volume rendering of large scientific data sets. In
*Proceedings of International Conference on Information Visual-
ization* (2005), pp. 259–267. 5
- [WS06a] WANG C., SHEN H.-W.: LOD map - a visual interface
for navigating multiresolution volume visualization. *IEEE Trans-
actions on Visualization and Computer Graphics* 12, 5 (2006),
1029–1036. 5, 6
- [WS06b] WOODRING J., SHEN H.-W.: Multi-variate, time-
varying, and comparative visualization with contextual cues.
IEEE Transactions on Visualization and Computer Graphics 12,
5 (2006), 909–916. 15
- [WS09] WOODRING J., SHEN H.-W.: Semi-automatic time-
series transfer functions via temporal clustering and sequencing.
Computer Graphics Forum 28, 3 (2009), 791–798. 9
- [WVG92] WILHELMS J., VAN GELDER A.: Octrees for faster
isosurface generation. *ACM Transactions on Graphics* 11, 3
(1992), 201–227. 4
- [WVG94] WILHELMS J., VAN GELDER A.: Multi-dimensional
trees for controlled volume rendering and compression. In *Pro-
ceedings of IEEE Symposium on Volume Visualization* (1994),
pp. 27–34. 4
- [WYG*11] WANG C., YU H., GROUT R. W., MA K.-L., CHEN
J. H.: Analyzing information transfer in time-varying multivari-
ate data. In *Proceedings of IEEE Pacific Visualization Symposium*
(2011), pp. 99–106. 7
- [WYM10] WANG C., YU H., MA K.-L.: Application-driven
compression for visualizing large-scale time-varying data. *IEEE
Computer Graphics and Applications* 30, 1 (2010), 59–69. 4
- [WYM13] WANG Y., YU H., MA K.-L.: Scalable parallel
feature extraction and tracking for large time-varying 3D volume
data. In *Proceedings of Eurographics Symposium on Parallel
Graphics and Visualization* (2013), pp. 17–24. 9
- [XS10] XU L., SHEN H.-W.: Flow web: A graph based
user interface for 3D flow field exploration. In *Proceedings
of IS&T/SPIE Conference on Visualization and Data Analysis*
(2010). 7, 9
- [YLRC10] YU L., LU A., RIBARSKY W., CHEN W.: Automatic
animation for time-varying data visualization. *Computer Graph-
ics Forum* 29, 7 (2010), 2271–2280. 15
- [YWM07] YU H., WANG C., MA K.-L.: Parallel hierarchical
visualization of large time-varying 3D vector fields. In *Proced-
ings of ACM/IEEE Conference on Supercomputing* (2007). 4, 9
- [YWM08] YU H., WANG C., MA K.-L.: Massively parallel vol-
ume rendering using 2-3 swap image compositing. In *Proced-
ings of ACM/IEEE Supercomputing Conference* (2008). 5
- [ZT09] ZHOU J., TAKATSUKA M.: Automatic transfer function
generation using contour tree controlled residue flow model and
color harmonics. *IEEE Transactions on Visualization and Com-
puter Graphics* 15, 6 (2009), 1481–1488. 11

Biography

Chaoli Wang is currently an associate professor of com-
puter science and engineering at University of Notre Dame.
He received a Ph.D. degree in computer and information sci-
ence from The Ohio State University in 2006. He was a post-
doctoral researcher at University of California, Davis from
2007 to 2009, and an assistant professor of computer science
at Michigan Technological University from 2009 to 2014.
Dr. Wang’s main research interest is scientific visualization,
in particular on the topics of time-varying multivariate data
visualization, flow visualization, and information-theoretic
algorithms and graph-based techniques for big data analyt-
ics. He has published extensively in visual analysis of scienti-
fic data sets leveraging various tree and graph representa-
tions. Dr. Wang is a recipient of the U.S. National Science
Foundation CAREER Award.